Data-driven Control of DC-DC Boost Converters Interfaced with Constant Power Loads

Behdad Moradi[1], Kamran Moradi[1], Pavol Bauer[2], *Senior Member, IEEE*, and Qobad Shafiee[1, 2], *Senior Member, IEEE*

[1]*Department of Electrical Engineering, University of Kurdistan,* Sanandaj, Iran

[2]*Department of Electrical Sustainable Energy, Delft University of Technology,* Delft, Netherlands

[1](behdad.moradi, k.moradi, q.shafiee)@uok.ac.ir, [2]p.bauer@tudelft.nl

2025 IEEE Seventh International Conference on DC Microgrids (ICDCM) | 979-8-3315-1274-3/25/$31.00 ©2025 IEEE | DOI: 10.1109/ICDCM63994.2025.11144662

***Abstract*—This paper presents a data-driven control framework to improve the stability and optimize the performance of DC-DC boost converters supplying constant power loads (CPLs). The inherent negative impedance and non-linear characteristics of CPLs pose significant stability challenges in power electronic systems. To address these issues, this study evaluates the performance of data-driven integrator (I) and linear quadratic integral (LQI) controllers, both optimized using iterative feedback tuning (IFT), that eliminates the need for an explicit system model. The proposed controllers are systematically compared against conventional model-based designs to assess their effectiveness. Key dynamic challenges, including converter non-linearity, CPL-induced instability, and measurement noise, are considered in the analysis. Simulation results demonstrate that the data-driven LQI and I controllers achieve superior tracking accuracy, robustness, and stability. These findings underscore the advantages of data-driven control methodologies in ensuring reliable and efficient operation in practical power electronic applications.**

***Index Terms*—Boost converter, constant power load, data-driven control, iterative feedback tuning, linear quadratic integral controller, microgrid.**

I. Introduction

The rapid expansion of microgrids (MGs) incorporating renewable energy sources (RESs), energy storage systems (ESSs), and power electronic converters necessitates advanced control strategies to ensure efficient, reliable, and stable operation. Recent research has emphasized the adoption of DC microgrids owing to their demonstrated efficacy in mitigating AC/DC conversion losses [1]. MGs are inherently complex, characterized by dynamic interactions among distributed components, nonlinearities, and frequent load fluctuations. In DC MGs, boost converters play a crucial role as power electronic interfaces, facilitating voltage regulation for applications such as photovoltaic (PV) systems, energy storage systems (ESSs), and electric vehicles (EVs). When supplying CPLs, these converters exhibit increased instability due to the negative impedance characteristics of CPLs, which intensify system nonlinearity and degrade control performance [2].

DC MG control techniques have been developed for multiple purposes, such as eliminating the need for demand-side grid synchronization, enabling compensation for disparities between power production and consumption through the integration of energy storage systems, preventing the load from being affected by harmonics and voltage sags or swells, and ensuring that voltage quality remains unaffected by current surges [3].

MGs require accurate modeling for control design and multi-timescale analysis. While simple models may suffice for linear control, precise modeling becomes essential when implementing advanced control strategies [4]. As distributed power supplies are increasingly utilized in isolated power systems, CPLs have grown to constitute a larger share of these systems. With the rapid proliferation of power electronics devices, the presence of CPLs is increasing significantly, profoundly impacting the stability of small-scale power systems due to their negative impedance characteristics [5]–[8].

DC-DC converters, particularly those with voltage boost capabilities, play a critical role as power electronic interfaces in DC MGs, elevating input voltage to higher levels through high-frequency switching. Among the common loads connected to these converters, power electronic converter loads, when tightly regulated, exhibit CPLs behavior [9]. Various control strategies have been explored for voltage and current regulation of boost converter with CPLs, as well as stabilization, in DC-DC converters, including proportional-integral (PI), fuzzy logic (FL), sliding mode control (SMC), state-dependent Riccati equation (SDRE), model predictive control (MPC) control, and etc., [10]–[14]. Implementing MPC for a boost converter with a CPL [14], [15] is challenging due to nonlinear dynamics, instability from negative impedance, high computational cost, modeling complexity, parameter sensitivity, and tuning difficulties, making simpler or data-driven controls preferable. The destabilizing effect of CPLs challenges classical model-based control approaches, which often struggle to achieve satisfactory stabilization performance [16]. Consequently, developing a robust nonlinear and linear control strategy to ensure the stability of load-side power equipment operation becomes a crucial endeavor. High-tech processors, advanced measurement devices for predicting voltage and current, and precise system modeling are significant challenges that data-driven control methods are well-equipped to overcome.

This paper proposes data-driven integrator (DDI) and data-driven linear quadratic integral (DDLQI) control methods to address the aforementioned challenges and enhance the efficiency of boost converters operating with CPLs. The employed data-driven technique, known as iterative feedback

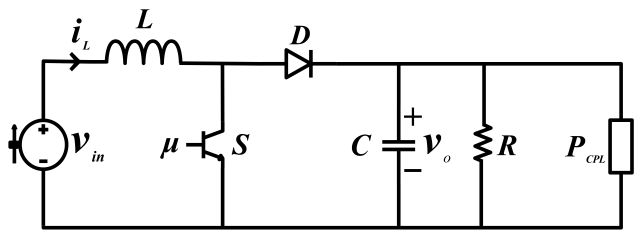

Fig. 1. Circuit topology of a dc-dc boost converter with a CPL.

tuning (IFT) [17], iteratively refines controller gains based on system voltage and current measurements collected during closed-loop operation [18], [19]. The IFT algorithm iteratively tunes I and LQI gains for precise voltage tracking under CPL condition, using only voltage and current data—no model needed, only a reference signal generation strategy is required. The effectiveness of the proposed data-driven control approach demonstrates significant effectiveness in power electronic systems [20], [21].

The key contribution of this work is a data-driven control framework that dynamically optimizes controller parameters in real time using direct voltage measurements, bypassing the need for an explicit system model. Simulation results demonstrate that this approach improves stability, convergence speed, and reference tracking accuracy over conventional model-based methods. The data-driven technique enhances settling time, robustness under load and parameter variations, and adaptability to uncertain dynamics outperforming traditional controllers in scenarios where precise modeling is difficult. These results highlight the effectiveness of the proposed method for complex or poorly characterized power electronic systems, where traditional model-based approaches may struggle.

The remainder of the paper is organized as follows. Section II presents the modeling and analysis of the boost converter with a CPL. Section III details the conventional control strategy, which form the basis for the proposed DDI and DDLQI methods introduced in Section IV. The simulation results under different scenarios are given in Section V. Finally, concluding remarks are provided in Section VI.

II. Modeling and Analysis

The schematic diagram of a DC-DC boost converter with a CPL is shown in Fig. 1. To derive the equations of the boost converter with a CPL in the continuous-time domain for the switching dynamics, first consider the case when switch S is closed (ON state). The circuit dynamics are described by:

$$\begin{cases} i_C = C\dfrac{dv_o}{dt} = -\dfrac{v_o}{R} - \dfrac{P_{CPL}}{v_o} \\ v_L = L\dfrac{di_L}{dt} = v_{in} \end{cases} \tag{1}$$

where L, C, and R are the inductance, capacitance, and resistor, respectively. v_{in}, v_o, and v_L are input, output, and inductor voltage of converter. i_C, i_L, and P_{CPL} are the capacitance current, instantaneous inductor current, and power value of CPL. When the switch S is opened (OFF state), the circuit dynamics are described by:

$$\begin{cases} i_C = C\dfrac{dv_o}{dt} = i_L - \dfrac{v_o}{R} - \dfrac{P_{CPL}}{v_o} \\ v_L = L\dfrac{di_L}{dt} = v_{in} - v_o \end{cases} \tag{2}$$

The averaged dynamic model of the boost converter with applying state-space averaging method yields the nonlinear averaged model, which can be expressed in the following form:

$$\begin{cases} L\dfrac{di_L}{dt} = v_{in} - (1-\mu)v_o \\ C\dfrac{dv_o}{dt} = (1-\mu)i_L - \dfrac{v_o}{R} - \dfrac{P_{CPL}}{v_o} \end{cases} \tag{3}$$

where μ is the duty cycle. The nonlinear averaged model requires small-signal linearization for control design, achieved by perturbing around the operating point [4]. The derivation begins by replacing all variables with the superposition of their steady-state values and small-signal perturbations:

$$\begin{aligned} \mu &= D + \hat{\mu}, \quad |\hat{\mu}| \ll D \\ v_o &= V_o + \hat{v}_o, \quad |\hat{v}_o| \ll V_o \\ i_L &= I_L + \hat{i}_L, \quad |\hat{i}_L| \ll I_L \end{aligned} \tag{4}$$

where D, V_o, and I_L are the steady-state of duty cycle, output voltage, and inductor current. Assuming constant input voltage $v_{in} = V_{in}$, the steady-state operating point and quiescent values are given by the steady-state analysis:

$$\begin{cases} I_L = \dfrac{P_{CPL}}{(1-\mu)V_o} + \dfrac{V_o}{(1-\mu)R} = \dfrac{V_{in}}{(1-\mu)^2 R} + \dfrac{P_{CPL}}{V_{in}} \\ V_o = \dfrac{V_{in}}{1-\mu} \end{cases} \tag{5}$$

The small-signal model of the CPL term is obtained via first-order Taylor series expansion:

$$\frac{P_{CPL}}{v_o} \approx \frac{P_{CPL}}{V_o} - \frac{P_{CPL}}{V_o^2}\hat{v}_o \tag{6}$$

Therefore, the small-signal state-space model of the boost converter with CPL is obtained as:

$$\frac{d}{dt}\begin{bmatrix} \hat{i}_L \\ \hat{v}_o \end{bmatrix} = \begin{bmatrix} 0 & -\dfrac{1-D}{L} \\ \dfrac{1-D}{C} & -\dfrac{1}{RC} + \dfrac{P_{CPL}}{CV_o^2} \end{bmatrix}\begin{bmatrix} \hat{i}_L \\ \hat{v}_o \end{bmatrix} + \begin{bmatrix} \dfrac{V_o}{L} \\ \dfrac{I_L}{C} \end{bmatrix}(1-\mu) \tag{7}$$

This linearized model enables rigorous stability analysis and control design while preserving the essential nonlinear effects of the original system.

III. Conventional Control Strategy

This section explores a conventional control strategy for boost converters with CPLs, focusing on the LQI controller. The LQI control scheme is designed to effectively regulate system dynamics while maintaining stability and performance across varying operating conditions.

A. Linear Quadratic Integral Controller

The LQI controller enhances LQR by adding integral action to eliminate steady-state error while optimizing performance. For boost converters with CPLs, it minimizes a cost function to balance transient response and control effort, ensuring robustness under dynamic conditions. Compared to classic controllers like PI, LQI achieves faster settling, reduced overshoot, and superior transient performance in high-power applications like renewable energy systems (RESs) and EVs, where precise voltage regulation is critical [22].

To design a continuous-time LQI controller, an integral state variable is introduced to eliminate steady-state error, defined as:

$$x_i(t) = \int e(t)\,dt, \quad \dot{x}_i(t) = e(t). \tag{8}$$

The augmented state vector combines the original state $x(t)$ and integral state $x_i(t)$:

$$x_{aug}(t) = \begin{bmatrix} x(t) \\ x_i(t) \end{bmatrix} = \begin{bmatrix} \hat{i}_L \\ \hat{v}_o \\ x_i \end{bmatrix}. \tag{9}$$

The augmented state-space representation is:

$$\begin{bmatrix} \dot{x}(t) \\ \dot{x}_i(t) \end{bmatrix} = \begin{bmatrix} A & 0 \\ -C & 0 \end{bmatrix} \begin{bmatrix} x(t) \\ x_i(t) \end{bmatrix} + \begin{bmatrix} B \\ 0 \end{bmatrix} u(t) + \begin{bmatrix} 0 \\ 1 \end{bmatrix} r(t), \tag{10}$$

where $C = [0\ \ 1]^T$ selects the output voltage from the system's state-space representation. This formulation extends the converter dynamics with integral action for precise voltage regulation. The LQI controller optimizes a cost function that balances the augmented state and control input:

$$J = \int_0^\infty \left(x_{aug}^T(t) Q x_{aug}(t) + u^T(t) R u(t) \right) dt, \tag{11}$$

where $u(t)$ is the control input, $Q \in \mathbb{S}_+^{n+p}$ and $R \in \mathbb{S}_+^m$ are weighting matrices to minimize the cost function, with $Q = \text{diag}([q_1, \ldots, q_n, q_{i1}, \ldots, q_{ip}])$ and $R = r$. For the boost converter with a CPL, the weighting matrices are tuned to balance the inductor current, output voltage, and integral error, where the $Q_{LQI} = \text{diag}([1, 1, 10^4])$ is tuned to prioritize zero steady-state error against CPL disturbances by heavily penalizing the integral error term, while $R_{LQI} = 10^4$ constrains the control effort to ensure practical implementation. The optimal control law for the LQI controller is given by:

$$u(t) = -K x_{aug}(t) = -\begin{bmatrix} K_x & K_i \end{bmatrix} \begin{bmatrix} x(t) \\ x_i(t) \end{bmatrix}, \tag{12}$$

where the gain matrix $K_{LQI} = [K_x\, K_i]$, with $K_x = [0.0290, 0.0045]$ and $K_i = -1$, is computed by solving the optimal control law equation using Q_{LQI} and R_{LQI}. The resulting closed-loop system provides improved transients and balance between tracking performance and stability for the boost converter's nonlinear dynamics.

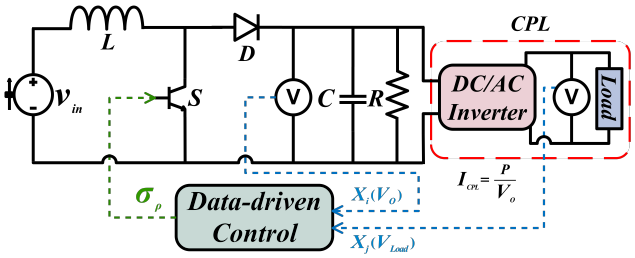

Fig. 2. A dc-dc boost converter with a CPL equipped with the proposed data-driven method.

IV. Data-driven Control Strategy

This section examines two data-driven control methods for boost converters with CPLs: the DDI and DDLQI controllers. These approaches utilize real-time system data to dynamically adjust control parameters, delivering enhanced stability, and optimized performance across varying operating conditions. As shown in Fig. 2, the proposed methodology involves conducting a series of experiments to implement the data-driven control design. The approach begins by generating a sequence of values for the state X which is measured output and load voltage at each sampling instant, the state σ, which serves as a control signal in each iteration. After gathering the experimental data, it is organized into the following matrices:

$$X = [x_0\, x_1\ \ldots\ x_\rho], \quad \sigma = [\sigma_0\, \sigma_1\ \ldots \sigma_\rho], \tag{13}$$

where ρ denotes the index of each experiment, ρ is an integer such that $1 \le \rho \le n$. With X_ρ and σ_ρ representing the state and input, respectively, for the ρ-th sampling. In this paper, the IFT method is used as a data-driven offline approach to optimally tune the controller parameters based on the output and load voltage, for controlling the voltage loop of the converter.

A. Data-driven Integrator Controller

The DDI controller enhances basic I controller by dynamically adjusting the integral gain of conventional I controller ($K_i I$) using system data. Instead of fixed gains, it employs IFT to optimize $K_i I$ in real time. The IFT minimizes a cost function to ensuring stability and performance under varying conditions. The controller continuously tunes $K_i I$ via voltage error feedback to ensure parametric robustness. The IFT process begins by defining the cost function to evaluate tracking error. The error between the achieved output $y(t, p)$ and the desired reference $r(t)$ is given by:

$$\hat{y}(t, p) = y(t, p) - r(t), \tag{14}$$

where p represents the controller parameter K_i, and the control objective is formulated as the minimization of the objective function:

$$J(p) = \frac{1}{2N} \sum_{t=1}^{N} E[\hat{y}(t, p)^2], \tag{15}$$

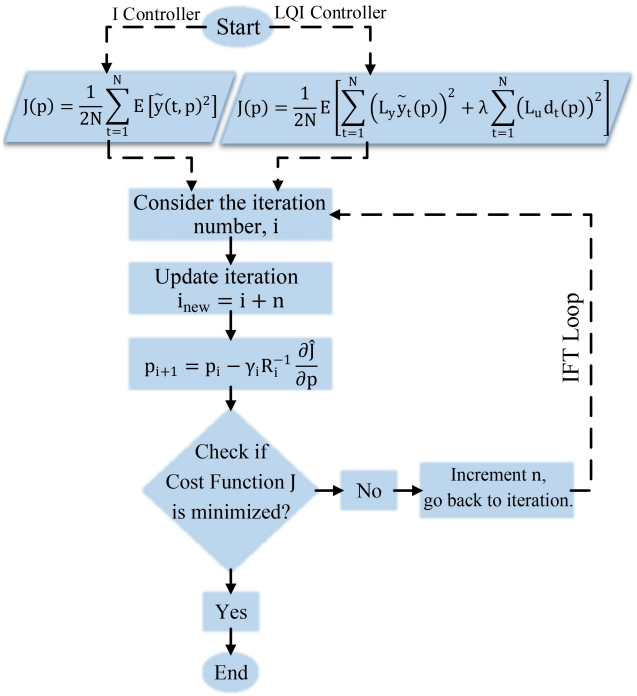

Fig. 3. Flowchart of the IFT-based DDI and DDLQI controller gain tuning process.

where N is the number of data points, and $E[\cdot]$ denotes the expectation operator for stochastic disturbances in the system. To minimize $J(p)$, a quasi-Newton method is employed, using gradient-based minimization. The parameter update rule is:

$$p_{i+1} = p_i - \gamma_i R_i^{-1} \frac{\partial J}{\partial p}(p_i), \tag{16}$$

where γ_i is the step size, R_i is an approximate positive definite matrix, and $\frac{\partial J}{\partial p}(p_i)$ is the gradient of the cost function at iteration i. The gradient is computed as:

$$\frac{\partial J}{\partial p}(p) = \frac{1}{N}\sum_{t=1}^{N}\left[\hat{y}(t,p)\frac{\partial \hat{y}}{\partial p}(t,p)\right], \tag{17}$$

where $\frac{\partial \hat{y}}{\partial p}(t,p)$ represents the sensitivity of the error is obtained by three-step experimental methodology: (1) perform a normal experiment with controller $C(p)$ and reference r, collecting N measurements of the output $y(p)$, denoted as $y^{(1)}(p)$; (2) perform a gradient experiment with reference $r - y^{(1)}(p)$, injecting this signal into the control variable output by $C(p)$, and collecting the output as $y^{(2)}(p)$; (3) approximate the gradient as:

$$\frac{\partial \hat{y}}{\partial p}(p) = \frac{\partial C}{\partial p}(p) y^{(2)}(p). \tag{18}$$

The matrix R_i, which influences the convergence speed, is approximated using the Gauss-Newton direction:

$$R_i = \frac{1}{N}\sum_{t=1}^{N}\frac{\partial \hat{y}}{\partial p}(p_i)\left(\frac{\partial \hat{y}}{\partial p}(p_i)\right)^T, \tag{19}$$

where a small $\hat{y}$ suggests $R_i \approx W$, which W is a positive definite matrix and helps ensure convergence by providing a well-conditioned update direction. The IFT logic for tuning the integrator controller gain, illustrated in Fig. 3, begins by defining the cost function and initializing the iteration counter $i = 1$. The parameter update for K_i is:

$$K_i^{(i+1)} = K_i^{(i)} - \gamma_i R_i^{-1}\frac{\partial J}{\partial K_i}, \tag{20}$$

where $K_i^{(i)} = 0.65$ initially, and γ_i is chosen as $\gamma_i = \frac{0.55}{i}$. The algorithm iteratively updates K_i by minimizing $J(p)$, and the optimization process is demonstrated across iterations using simplified gradient and Hessian values (experimentally computed in practice) for illustration.

The cost function decreased from $J(p^{(1)}) = 5.2$ to $J(p^{(4)}) = 4.5$ in 4 iterations, indicating improved accuracy and system steadiness. The algorithm converges when $|J(i) - J(i-1)| < \epsilon$, which $\epsilon = 0.55$. The proposed method successfully fine-tunes the integral gain K_i, achieving an optimized value of $K_i DDI = 0.8117$ from an initial setting of $K_i I$. This technique ensures reliable operation in challenging environments with nonlinear dynamics, enhancing the overall efficiency of power conversion systems.

B. Data-driven Linear Quadratic Integral Controller

The DDLQI controller enhances LQI control by iteratively tuning the weighting matrices Q_{LQI} and R_{LQI}. The parameters are combined into $p = [q_1, q_2, q_3, r]^T$, which is iteratively optimized to balance voltage regulation and control effort. Using real-time output voltage and error data, the controller adjusts $Q_{LQI} = \text{diag}([1, 1, 10^4])$ and $R_{LQI} = 10^4$. The IFT-based optimization as in Section IV-A minimizes a cost function evaluating both tracking error and control input. The control objective minimizes a cost function that balances tracking error and control effort:

$$J(p) = \frac{1}{2N}E\left[\sum_{t=1}^{N}\left(L_y\hat{y}_t(p)\right)^2 + \lambda\sum_{t=1}^{N}\left(L_u d_t(p)\right)^2\right], \tag{21}$$

where L_y is the output filter, designed for reference tracking and tracking error frequencies, while L_u is the input filter, which constrains the control signal bandwidth. Both L_y and L_u act as weighting matrices, optimizing the trade-off between performance and robustness through frequency-selective weighting. The $d_t(p)$ represents the control effort influenced by Q and R, and λ adjusts the trade-off between error minimization and control effort. The IFT process employs a quasi-Newton optimization method, using the parameter update rule. The gradient of the cost function is:

$$\frac{\partial J}{\partial p}(p) = \frac{1}{N}\sum_{t=1}^{N}\left[L_y^2\hat{y}_t(p)\frac{\partial \hat{y}_t}{\partial p}(p) + \lambda L_u^2 d_t(p)\frac{\partial d_t}{\partial p}(p)\right], \tag{22}$$

where sensitivities $\frac{\partial \hat{y}_t}{\partial p}(p)$ and $\frac{\partial d_t}{\partial p}(p)$ are estimated experimentally and convergence matrix R_i ensures stability as in Section IV-A. Fig. 3 shows the IFT-based DDLQI optimization and tuning the controller gain. The step size optimization is $\gamma_i = \frac{0.1}{i}$, and the parameter update rule is given by:

$$p^{(i+1)} = p^{(i)} + \gamma_i R_i^{-1} \frac{\partial J}{\partial p}\Big|_{p=p^{(i)}}, \tag{23}$$

where $R_i = \text{diag}([r_{i,1}, r_{i,2}, r_{i,3}, r_{i,4}])$ is a diagonal preconditioning matrix, and $\frac{\partial J}{\partial p}$ is the gradient.

From iterations 1 to 6 with starting from the initial parameter vector $p^{(1)} = [1,\ 1,\ 10^4,\ 10^4]^T$, the iterative optimization reduced the gradient norm from 1921 to 58. Correspondingly after six iterations, further updates yield minimal improvement, so the cost function decreased from $J(p^{(1)}) = 5.2$ to $J(p^{(6)}) = 4.05$. The algorithm was considered converged when the change in cost between iterations satisfied $|J(i) - J(i-1)| < \epsilon$ with a predefined threshold $\epsilon = 0.1$. The optimized DDLQI parameters are $Q_{DDLQI} \approx \text{diag}([1.1927,\ 1.1582,\ 10^4])$, $R_{DDLQI} \approx 10^4$, and $K_{DDLQI} = [0.0358,\ 0.00590,\ -1]$. The DDLQI controller adaptively tunes Q_{LQI} and R_{LQI} to ensuring robust voltage regulation in CPLs applications. The IFT-based optimization adaptively tunes both I and LQI gains, enhancing stability and transient response across varying operating conditions while maintaining consistent output regulation.

V. Simulation Results

Simulations evaluate and compare the I, DDI, LQI, and DDLQI controllers for a boost converter with a CPL, under varying input voltages ($V_{in} = 13, 14, 15\ V$), and load change ($R = 20, 30, 40\ \Omega$). These test verify the controller's ability to maintain stable operation during input and load variations, ensure fast and smooth transients, and steady-state stability across conditions. The parameters of the converter and controller are provided in Table I.

TABLE I
Converter and Control Parameters

Parameter	Symbol	Value
Converter Parameters		
Input Voltage	V_{in}	12 V
Reference Voltage	V_{ref}	24 V
Constant Power Load	P_{CPL}	10 W
Inductance	L	1 mH
Capacitance	C	100 µF
Resistance	R	50 Ω
Switching Frequency	f_{sw}	100 kHz
Control Parameters		
I Controller Gain	K_iI	0.65
DDI Controller Gain	K_iDDI	0.8117
LQI Tracking Error	Q_{LQI}	$[1, 1, 10^4]$
LQI Control Effort	R_{LQI}	10^4
DDLQI Tracking Error	Q_{DDLQI}	$[1.1927, 1.1582, 10^4]$
DDLQI Control Effort	R_{DDLQI}	10^4

A. Normal Case

For $V_{\text{in}} = 12V$ and $R = 50\,\Omega$, the comparative analysis reveals that the DDI controller demonstrates faster settling time ($t_s = 0.14s$ vs $0.19s$) and reduced overshoot compared to the conventional I controller in Fig. 4, while maintaining better steady-state accuracy. Similarly, Fig. 5 shows the DDLQI controller achieves better reference tracking and improved disturbance rejection compared to standard LQI, particularly during the transient phase (0.1s–0.2s).

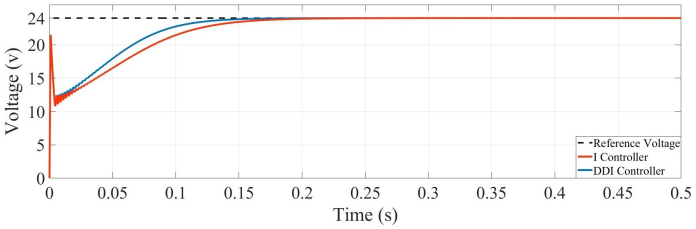

Fig. 4. Output voltage tracking response of I and DDI controllers.

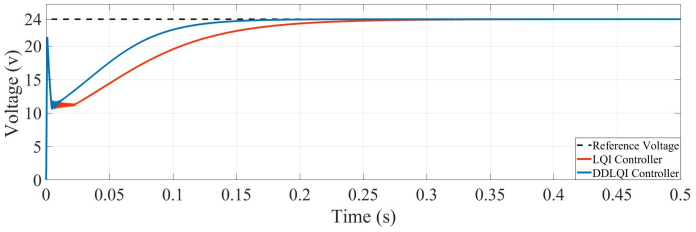

Fig. 5. Output voltage tracking response of LQI and DDLQI controllers.

B. Input Voltage Change

Varying V_{in} simulates conditions such as battery discharge or fluctuations in RESs, where the input voltage is not constant. The system response to input voltage steps, Fig. 6 (a) demonstrates the varying input voltage of system. When the input changes from $14V$ to $15V$ to $13V$ in $0.5s$ increments, Fig. 6 (b) shows that DDI and DDLQI controllers maintain better reference tracking accuracy than I and LQI controllers. At the $15V$ transition, all controllers experience brief oscillations, but DDI and DDLQI dampen these oscillations more rapidly. The most significant performance difference appears during the $13V$ transition, where conventional controllers exhibit more pronounced oscillations and longer settling times. The I and LQI controllers demonstrates the lowest overshoot, while the DDI and DDLQI controllers exhibit larger overshoot, they achieve significantly faster reducing settling time more than conventional controllers.

C. Load Change

Adjusting load variations with changing sequentially from $30\,\Omega$ to $40\,\Omega$ and then to $20\,\Omega$ every $0.5s$ tests the transient response of the controllers. As shown in Fig. 7, the DDLQI controller consistently maintains the tightest voltage regulation, outperforming the LQI and I controllers in minimizing voltage deviations during load changes. The DDI controller demonstrates a faster settling time compared to the I controller, while both DDI and DDLQI effectively suppress the oscillations observed in the I and LQI controller responses following each load transition. Similar to the input voltage variation case, both the I and LQI controllers demonstrate superior overshoot reduction compared to the data-driven counterparts.

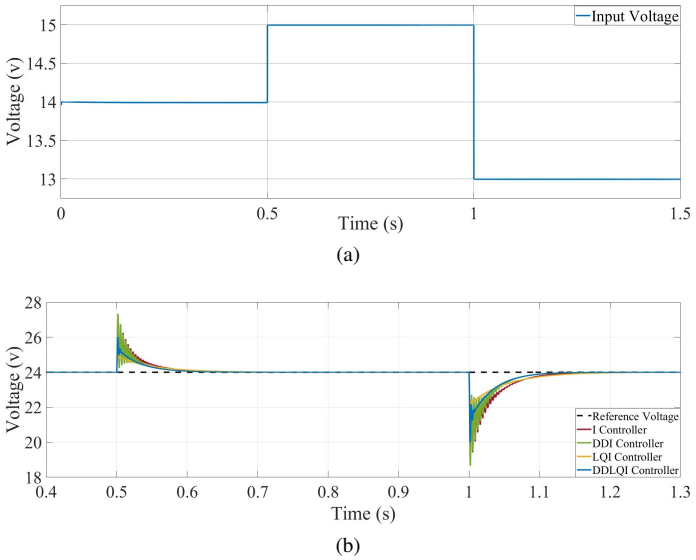

Fig. 6. (a) Input voltage step change at 0.5s intervals, (b) Performance of the proposed controllers under input voltage change.

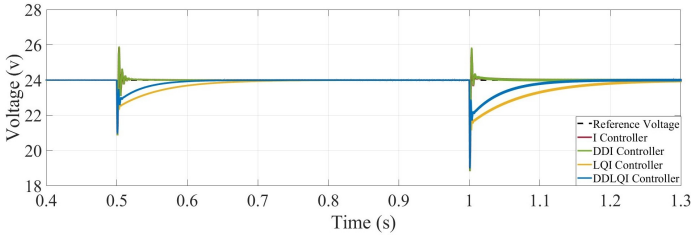

Fig. 7. Performance of the proposed controllers under load change.

VI. Conclusion

This work proposes data-driven IFT-based controllers DDI and DDLQI for boost converters with CPLs, overcoming limitations of model-based approaches I and LQI that require accurate system models vulnerable to parameter drift, unmodeled dynamics, and CPL negative impedance. By adaptively optimizing control gains through real-time voltage measurements, our method achieves enhanced disturbance rejection and robustness without system identification, demonstrating faster settling times and reliable voltage regulation during abrupt load and input changes, which is crucial for microgrids and power electronics with variable loads. While not always superior in overshoot reduction, the approach proves particularly valuable in scenarios with modeling challenges or frequent parameter variations, establishing a foundation for adaptive power electronics control with future potential in multi-objective optimization, energy efficiency integration, and scalable energy systems.

References

[1] T. Dragicevic, P. Wheeler, and F. Blaabjerg, *DC Distribution Systems and Microgrids*. London, U.K.: Inst. Eng. Technol., 2018.

[2] Qobad Shafiee, Mobin Naderi, Hassan Bevrani, *Microgrid Dynamic Modeling: Concepts and Fundamentals, in Microgrids: Dynamic Modeling, Stability and Control*, IEEE, pp.15-78, 2024.

[3] Tabatabaei, N.M., Kabalci, E., Bizon, N., *Microgrid Architectures, Control and protection methods*, Springer, Cham, 2019.

[4] Qobad Shafiee, Mobin Naderi, Hassan Bevrani, *Microgrid Control: Concepts and Fundamentals, in Microgrids: Dynamic Modeling, Stability and Control*, IEEE, pp. 143-195, 2024.

[5] Emadi Ali, Fahimi Babak, Ehsani Mehrdad, *On the concept of negative impedance instability in the more electric aircraft power systems with constant power loads*, Society of Automotive Engineers (SAE) Journal, 1999.

[6] Jusoh Awang Bin, *The instability effect of constant power loads*, National Power and Energy Conference, pp. 175-179, 2004.

[7] E. Hossain, R. Perez, A. Nasiri, and S. Padmanaban, *A comprehensive review on constant power loads compensation techniques*, IEEE Access, vol. 6, pp. 33285-33305, 2018.

[8] W. He and R. Ortega, *Design and implementation of adaptive energy shaping control for DC–DC converters with constant power loads*, IEEE Trans. Ind. Informat., vol. 16, no. 8, pp. 5053–5064, 2020.

[9] M. Forouzesh, P. Y. Siwakoti, A. S. Gorji, F. Blaabjerg, and B. Lehman, *Step-up DC–DC converters: A comprehensive review of voltage boosting techniques, topologies, and applications*, IEEE Trans. Power Electron., vol. 32, no. 12, pp. 9143–9178, 2017.

[10] P. C. Papageorgiou and A. T. Alexandridis, *Output Current-based Voltage Regulation of CPLs fed by dc/dc Power Converters*, 6th IEEE International Energy Conference (ENERGYCon), Gammarth, Tunisia, pp. 734-739, 2020.

[11] M. K. Al-Nussairi and R. Bayindir, *DC-DC Boost Converter Stability with Constant Power Load*, 18th IEEE International Power Electronics and Motion Control Conference (PEMC), Budapest, Hungary, pp. 1061-1066, 2018.

[12] S. Barhoumi, A. Sahbani and K. Ben Saad, *Sliding Mode Control for a Boost converter with Constant Power Load*, 4th International Conference on Control Engineering Information Technology (CEIT), Hammamet, Tunisia, pp. 1-5, 2016.

[13] Z. Karami, Q. Shafiee, Y. Batmani, and H. Bevrani, *On the design of suboptimal controller for dc microgrids with cpl*, Energy Procedia, vol. 141, pp. 611–618, 2017.

[14] Z. Karami, Q. Shafiee, S. Sahoo, M. Yaribeygi, H. Bevrani and T. Dragicevic, *Hybrid Model Predictive Control of DC–DC Boost Converters With Constant Power Load*, in IEEE Transactions on Energy Conversion, vol. 36, no. 2, pp. 1347-1356, 2021.

[15] C. Zhang, M. Li, L. Zhou, C. Cui and L. Xu, *A Variable Self-Tuning Horizon Mechanism for Generalized Dynamic Predictive Control on DC/DC Boost Converters Feeding CPLs*, IEEE Journal of Emerging and Selected Topics in Power Electronics, vol. 11, no. 2, pp. 1650-1660, 2023.

[16] A. M. Rahimi and A. Emadi, *Discontinuous-conduction mode DC/DC converters feeding constant-power loads*, IEEE Trans. Ind. Electron., vol. 57, no. 4, pp. 1318–1329, 2010.

[17] H. Hjalmarsson, M. Gevers, S. Gunnarsson, O. Lequin, and A. Bouzid, *Iterative feedback tuning: theory and applications*, IEEE control systems magazine, vol. 18, no. 4, pp. 26–41, 1998.

[18] K. Moradi, H. Sheikhahmadi, P. Zamani, Q. Shafiee and H. Bevrani, *A Data-driven PI Control of Grid-Connected Voltage Source Inverters Interfaced with LCL Filter*, 13th Power Electronics, Drive Systems, and Technologies Conference (PEDSTC), Tehran, Iran, Islamic Republic of, pp. 645-650, 2022.

[19] P. Zamani, K. Moradi and Q. Shafiee, *Improving Maximum Power Point Tracking of PV Systems Using a Data-driven PI Control*, 11th Smart Grid Conference (SGC), Tabriz, Iran, Islamic Republic of, pp. 1-6, 2021.

[20] K. Moradi, P. Zamani, Q. Shafiee, *Data-driven predictive control of perturbed buck converters using a modified iterative feedback tuning algorithm*, IET Power Electron, vol. 17 no. 10, pp. 1314–1323, 2024.

[21] K. Moradi, P. Zamani and Q. Shafiee, *Data-driven Predictive Control of Buck Converters Under Load and Input Voltage Uncertainties*, 13th Power Electronics, Drive Systems, and Technologies Conference (PEDSTC), Tehran, Iran, Islamic Republic of, pp. 334-340, 2022.

[22] Sakasegawa E, Watanabe S, Shiraishi T, Haga H, Kennel RM, *A Novel LQI Control Technique for Interleaved-Boost Converters*, World Electric Vehicle Journal, vol. 15 no. 8, 2024.